Biointerface Research in Applied Chemistry
Open-Access Journal (ISSN: 2069-5837)

Article
Volume 13, Issue 1, 2023, 52
https://doi.org/10.33263/BRIAC131.052

Uridine-Derived 4-Aminophenyl 1-Thioglucosides: DFT Optimized FMO, ADME, and Antiviral Activities Study

Mohammad Atiqur Rahman [1], Unesco Chakma [2], Ajoy Kumer [3], Md. Rezaur Rahman [4], Mohammed Mahbubul Matin [1,*]

[1] Bioorganic and Medicinal Chemistry Laboratory, Department of Chemistry, Faculty of Science, University of Chittagong, Chittagong, 4331, Bangladesh; atiqchemcu@gmail.com (M.A.R.); mahbubchem@cu.ac.bd (M.M.M.);
[2] Department of Electrical and Electronic Engineering, European University of Bangladesh, Gabtoli, Dhaka, 1216, Bangladesh; unescochakma@gmail.com (U.C.);
[3] Department of Chemistry, European University of Bangladesh, Gabtoli, Dhaka, 1216, Bangladesh; ajoy@eub.edu.bd (A.K.);
[4] Department of Chemical Engineering and Energy Sustainability, Faculty of Engineering, Universiti Malaysia Sarawak, Jalan Datuk Mohammad Musa, Kota Samarahan, 94300, Malaysia; rmrezaur@unimas.my (M.R.M.);
* Correspondence: mahbubchem@cu.ac.bd (M.M.M.);

Scopus Author ID 7006284929
Received: 12.11.2021; Accepted: 16.12.2021; Published: 30.01.2022

Abstract: The biological roles of carbohydrates, especially their synthetic glycoconjugates, are at the forefront of research, and their applications and research are in the development of an impressive area of carbohydrate-derived vaccines. Considering this, several thioglucosides 2-6 conjugated with para-aminophenyl and uridine moieties are investigated for their possible application as hepatitis antiviral applications. Geometry optimization of these uridine thioglucosides by density functional theory (DFT) indicated that their glucopyranose rings are in $^4C_1$ chair conformation with β-glucosidic linkage. Frontier molecular orbital (FMO), molecular electrostatic potential (MEP), lower hardness, and softness calculations indicated their higher electrophilic nature. Solubility and ADMET studies indicated that the uridine thioglucosides might be safer drugs to use. With these encouraging results, molecular docking of 2-6 was conducted with hepatitis C virus (HCV, 3su4) and hepatitis B virus (HBV, 5e0i) proteases where the binding affinities for 2-6 were found higher than the standard anti-hepatitis drug sofosbuvir. Overall, the thioglucosides showed a better binding affinity with HBV protease (5e0i) than the HCV protease (3su4), indicating their prospect against these viruses.

Keywords: DFT optimization; docking; 5e0i; glucoconjugates; Hepatitis viral infection; pharmacokinetic properties; protease inhibition; 3su4.

1. Introduction

Changes in glycosylation can alter inflammatory responses, promote cancer cell metastasis and enable viral immune escape, including damage to kidney function that affects health problems and diseases. In this respect, glycoconjugation of selected monosaccharides/carbohydrates with chosen proteins and other biomolecules improve the ability to fine-tune immunological responses and boost immune responses to cancer. A sufficient fundamental understanding of glycoconjugates' structural insights and functions may enrich glycomedicine. Most glycoconjugate relies on a covalent link between carbohydrates and chosen molecule or macromolecule (protein) [1]. The biosynthesis of highly glycosylated glycoproteins found on the surface of several viruses is prepared by glycosyltransferases (GTs)

[2,3]. Thus, the GTs inhibitors can be used to control the growth of viruses. Many sugar-based glycoconjugates are intensively designed as new effective GT inhibitors. Of them, uridine-derived 1-thioglycosides, a new type of sugar nucleotides, were found to be potential GT inhibitors [4,5]. Also, carbohydrate-derived synthetic glycoconjugates are at the forefront of research, and their application and research are developing an impressive area of carbohydrate-derived vaccines.

Alkyl and acyl glycoses and glycoside derivatives/esters of sugars have shown potential biological activities [6-8], and hence, possess immense importance in bioorganic and medicinal chemistry. Protection/modification of a particular functional group of sugar residue is always used for the synthesis of new derivatives of substantial importance [9,10] in addition to the modification of the remaining functional groups in sugar molecule(s). Various methods for esterification/modification of sugars and sugar parts of nucleosides have so far been reported and employed successfully [11-15]. A plethora of sugar-based bioactive compounds possess aromatic and heteroaromatic nuclei. Our several reports described that incorporating an active nucleus to the monosaccharide moiety increased greater potentiality for biological activity for the resulting molecule/nucleus [16-19]. Incorporation of the benzene substituted benzene and heterocyclic nuclei served an important role as a common denominator for many biological functions [20-23].

Uridine (1), with ribofuranose sugar moiety, containing natural products are reported to exhibit a broader range of biological activities, like antifungal [24-26], anticancer, antiviral, and antibiotic activity, and are implicated in various metabolic pathways [27-30]. For example, several 4-*t*-butylbenzoyl uridine esters with different aliphatic and aromatic groups were synthesized and showed significant binding affinities against SARS-CoV-2 main protease (7BQY) [31]. It was also found to show asthmatic airway inflammation, anti-depression activity, and hepatocyte proliferation [32]. Sleep-promoting and anti-epileptic effects boost memory function with enhanced neuronal plasticity [33]. Uridine derivatives, especially its esters, showed many promising neuroprotective effects with increased 5-HT and 5-HIAA levels [34]. The carbohydrate glycoconjugates are used to treat pathogenic organisms *Mycobacteria* spp., *Leishmania* spp., *E. coli*, *T. cruzi*, and *Klebsiella* spp in mammals [35,36]. A series of uridine derivatives with methylene 1,2,3-triazole unit and/or an amide unit which connects the carbohydrate (glucose or galactose) and uridine moiety was synthesized, which showed higher activity against GTs [37].

Many therapeutic drugs in use (e.g., pegylated interferon) have numerous side effects [38], and extremely high costs cause low therapeutic access on a global scale [39]. Carbohydrate-derived therapeutic agents are biodegradable and cost-effective with minimum or no side effects [40]. Many reviews indicated that uridine (and its nucleotides) has crucial functions that help regulate various biological systems [41]. Uridine (1) and UDP-glucose have been used to reduce the undesired side effects and toxicity of pyrimidine-containing anticancer drugs [42]. In addition, some silyl-protected novel uridine-based glycoconjugates (with different linkers) are found potential antiviral *in vitro*, especially against hepatitis C virus (HCV; IC_{50} ~4.9-13.5 µM) and classical swine fever virus (CSFV; IC_{50} ~4.2 µM) with very low cytotoxicity [5]. Over 170 million people are infected by the Hepatitis C virus (HCV) worldwide and are the leading cause of chronic liver diseases, including cirrhosis, liver failure, and liver cancer. In this context, as well as our continuous effort in this field [43-45], several uridines based thioglucosides with *para*-aminophenyl moiety (Figure 1) have been considered for their antiviral efficacy against Hepatitis C (3su4) virus and extended/compared with

Hepatitis B (5e0i) virus. Uridine-based thioglucosides are structurally related to the standard HCV drug sofosbuvir. Correlations have been conducted for acyl groups among uridine, glucose, and both uridine-glucose units. In addition to molecular docking, drug-likeness properties ADME of these compounds have been discussed in this study.

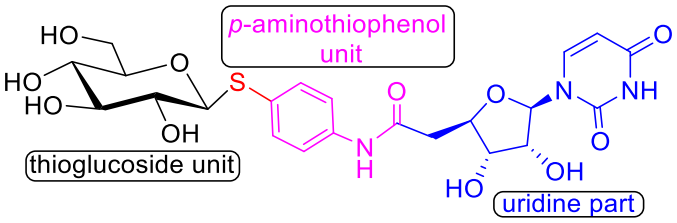

Figure 1. The general structure of uridine-based thioglucosides with *para*-aminophenyl moiety.

2. Materials and Methods

2.1. Materials.

In the present study, uridine (1), its 4-aminothiophenylglucoside 2, and acetate 3-6 are chosen (Figure 2). For the rigorous comparison, acetyl groups in uridine moiety (3-4), in glucoside moiety (5), and both moieties (6) are considered. Several of these compounds and related glucosides were synthesized by various researchers [4,5,37]. Structurally thioglucosides 2-6 contain an amido functional group, a pyrimidine ring, and pyranose and furanose rings. D-glucopyranose and uridine are linked together via *para*-aminothiophenol unit (Figure 2).

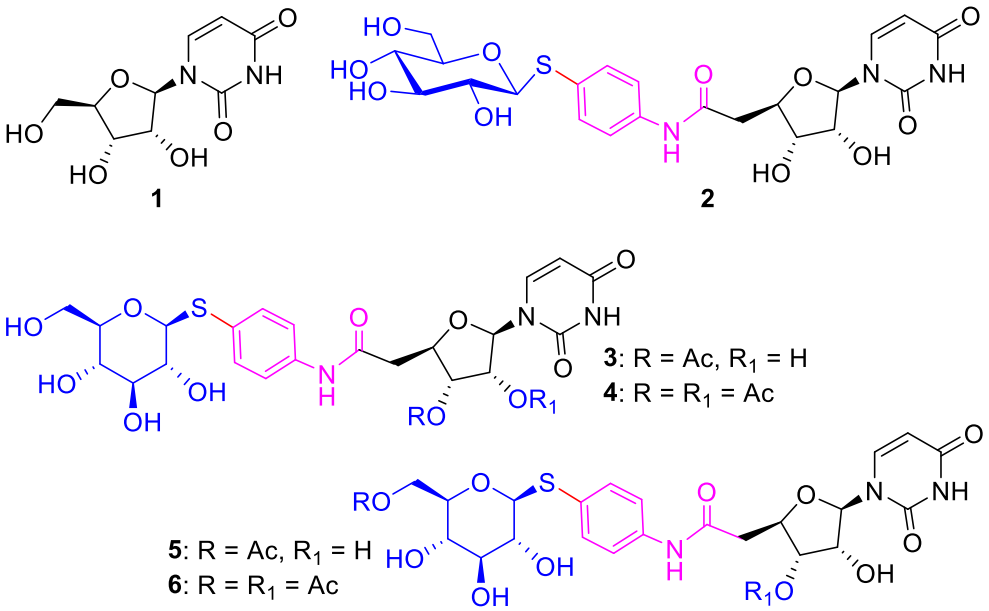

Figure 2. Structure of uridine (1) and its thioglucosides 2-6.

2.1. Methods

2.2.1. Optimization and chemical reactivity and descriptor calculation.

The basic geometry of glucopyranoside and uridine (1) was initially taken from the online structure database known as ChemSpider. Having these structures, the necessary molecules 2-6 with appropriate geometry were drawn in the GaussView (5.0) program [46]. All the thioglucosides and uridine compounds were then optimized with Gaussian 09 program at DFT (B3LYP) computing method [47] with a 3-21G* basis set [47-49]. It should be noted

that due to the larger molecular sizes, higher basis sets couldn't be used. For optimization, dry conditions at 298 K and 1 atm were maintained. The DFT optimized structures were used for the FMO (frontier molecular orbital) energy calculations like HOMO (highest occupied molecular orbital), LUMO (lowest unoccupied molecular orbital), and HOMO-LUMO gap, etc.

The magnitude of chemical reactivity and descriptors are calculated using related accepted equations. Such as- energy gap, $\Delta\varepsilon = \varepsilon LUMO - \varepsilon HOMO$; ionization potential, $I = -\varepsilon HOMO$; electron affinity, $A = -\varepsilon LUMO$; electronegativity, $\chi = (I+A)/2$; chemical potential, $\mu = -(I+A)/2$; hardness, $\eta = (I-A)/2$; electrophilicity, $\omega = \mu 2/2\eta$; softness, $S = 1/\eta$.

All the chemical reactivity descriptors are compared with the standard medication named sofosbuvir (brand name Sovaldi) used to treat the hepatitis C virus. DOS plots were obtained from GaussSum 3.0. Molecular electrostatic potential (MEP) was also calculated at the same level of DFT, and MEP calculation was conducted by an online WebMO demo server [44,50].

2.2.2. Calculation of ADMET and Lipinski rule.

Knowing structural features and chemical descriptors, these glucoconjugates were run on SwissADME online database (http://www.swissadme.ch) [51] for evaluating their Lipinski rule satisfaction. In addition, prediction of pharmacokinetic (PK) properties is generally conducted ahead of in vivo tests which tremendously reduce time and cost for drug discovery procedure. The ADMET properties were completed by the online database amdetSAR (http://biosig.unimelb.edu.au), the most acceptable database for predicting the AMDET parameters [52]. The optimized structures of 1-6 in InChIKey and SMILES formats were used for their ADMET calculation. For rigorous comparison, a standard hepatitis C drug, sofosbuvir was used.

2.2.3. Method for molecular docking.

Common antiviral drugs (telaprevir, danoprevir, vaniprevir) inhibit the HCV viral NS3/4A protease (PDB ID: 3su4). However, the sustainable applications of the common drug class are challenged by the quick emergence of resistance. Hence, potential strategies for developing robust therapies against this rapidly developing virus are essential. In addition, hepatitis B virus (HBV, a double-stranded DNA virus) inhibitors bound to HBV's core protein capsid Y132A (PDB ID: 5e0i) and found an important target for the antiviral drugs by inhibiting its replication. Based on the structural and mechanistic understanding, the selected uridine glycoconjugates are docked with 3su4 and 5e0i followed by comparing docking score with a standard antiviral drug (Sofosbuvir; approved for the treatment of chronic HCV infected patients).

Ligand preparation: For the ligand preparation, the DFT optimized structures (Section 2.2.1) were executed for the molecular optimization by utilizing vibrational frequency from the DMol3 code of Material Studio 08 [53]. The functional B3LYP and Basis set DNP+ were used from DMol3 code. Finally, the optimized ligands were exported as the PDB file for molecular docking study.

Protein preparation: The original three-dimensional (3D) crystal structure of Hepatitis C (3su4; Resolution: 2.25 Å) and Hepatitis B (5e0i; Resolution: 1.95 Å) viruses were collected from the RSCB Protein Data Bank (PDB) [54]. After taking the proteins from PDB, these were

viewed by the PyMOL software version using PyMOL V2.3 (https://pymol.org/2/) [55]. The crystal structure of the protease was adjusted and verified based on their lowest energy eliminated water molecules and was saved as PDB files. In the next step, the pdb file was energetically minimized in another software called Swisspdb.

Molecular docking: Molecular docking is mainly investigated to calculate the binding affinity with protein, bonding interaction, bonding mode in their mechanism for bonding between ligand and protein [56], which are the key factors to study biologically active compounds against pathogenic protein strains. The docking procedure was performed with the help of AutoDock Vina incorporated from PyRx Virtual Screening Tools. After loading ligands (compounds) and proteins, their energy is minimized and saved as pdbqt file format. Both the files are forwarded for docking. The grid center points were set in X = -6.0679 Å, Y =2.8496 Å, Z = 20.8678 Å, and the dimension in X = 74.8931 Å, Y = 57.6001Å, Z = 92.1773Å. The grid box dimensions were selected and set up to wrap the protein's substrate-binding region. The BIOVIA Discovery Studio Visualizer 2017 was used to analyze the non-covalent interaction between the ligands and the pathogenic protein [57].

3. Results and Discussion

3.1. Optimized structures of thioglucoside 2-6.

Molecular structure, conformation, and shape greatly influence their interactions with receptor proteins and their biological functionality [44]. Thus, initially, the molecular structures of these uridine-glycoconjugates are determined. As shown in Figure 3, the glucoconjugates 2-6 glucopyranose rings exist in $^4C_1$ chair conformation in β-thioglucosidic linkage.

In compounds 2-6, the ribofuranose part of uridine is attached to the pyrimidine ring with β-linkage. Interestingly, the primary hydroxyl group or its acetyl group of glucopyranose unit and CO/NH of pyrimidine unit of 2-6 are found closer/*cis* to each other (Figure 3). Thioglucosidic bond angle (∠C1-S-C) was found 101.3-101.6° and ribose to amide (∠C4′-C5′-CO) 110.6-111.9° for compound 2-4. Whereas, attachment of C-6 acetyl group at glucopyranose unit, as in 5-6, reduced both the bond angles (98.2-98.7° and 109-109.6°, respectively). This is probably due to the attractive force between the acetyl carbonyl oxygen and the nitrogen atom of the pyrimidine ring.

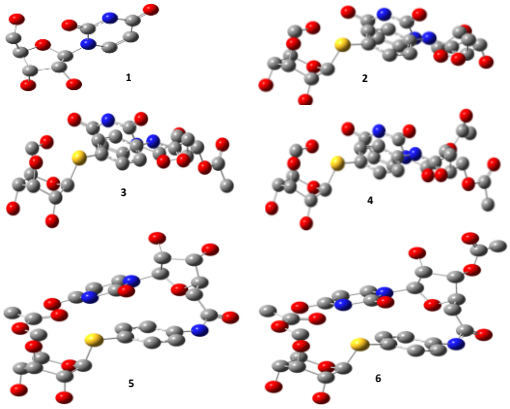

Figure 3. DFT optimized structure of thioglucoside **2-6** (H atoms are not shown).

3.2. Molecular orbitals and chemical reactivity descriptors.

The chemical descriptors generally carry a special significance for any organic compound or biologically active molecule. The magnitude of εLUMO, εHOMO, and energy

gap (Δε), ionization potential (I), electron affinity (A), chemical potential (μ), electronegativity (χ), hardness (η), electrophilicity (ω) and softness (S) of the six molecules 1-6 are presented in Table 1. These data were calculated by the DFT function.

Table 1. Frontier molecular orbitals and reactivity descriptor analysis of 1-6.

Mol	εLUMO (eV)	εHOMO (eV)	Δε (eV)	I (eV)	A (eV)	μ (eV)	η (eV)	χ (eV)	ω (eV)	S (eV)
1	-1.425	-9.592	8.167	9.592	1.425	-5.508	4.083	5.508	3.715	0.244
2	-1.462	-8.734	7.272	8.734	1.462	-5.098	3.636	5.098	3.573	0.275
3	-1.987	-8.303	6.316	8.303	1.987	-5.145	3.158	5.145	4.191	0.316
4	-2.301	-8.246	5.945	8.246	2.301	-5.273	2.972	5.273	4.677	0.336
5	-1.372	-7.997	6.625	7.997	1.372	-4.684	3.312	4.684	3.312	0.301
6	-1.638	-8.571	6.933	8.571	1.638	-5.104	3.466	5.104	3.758	0.288
SB	-0.198	-9.338	9.140	9.338	0.198	-4.768	4.570	4.768	2.487	0.218

Mol = molecule (compound); LUMO = lowest unoccupied molecular orbital; HOMO = highest occupied molecular orbital; SB = sofosbuvir (standard antiviral drug).

It is evident from Table 1 that both uridine and sofosbuvir possess a similar HOMO-LUMO gap (Δε). Whereas, all the glucoconjugates 2-6 had lower Δε values than the uridine (1), which indicated their better chemical reactivities. It should be noted that the smaller the energy gap Δε, the greater the reactivity for a molecule [46,48,58]. The higher electrophilicity index ω values for 1-6 (3.7-4.2 eV) than sofosbuvir (2.5 eV) indicated them as stronger electrophiles than the standard drug. The addition of acetyl group in the uridine thioglycosides, as in 3-6, gradually decreased their hardness and increased softness compared to uridine (1) and sofosbuvir, indicating their more reactive nature (according to the maximum hardness principle). DOS plot indicating HOMO-LUMO gap (Δε) of 5 and 6 are shown in Figure 4.

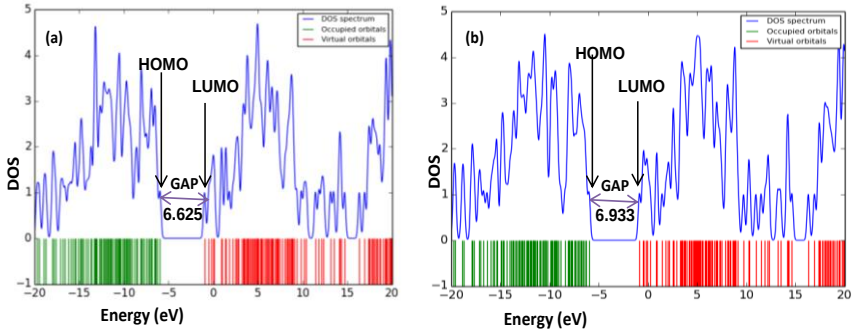

Figure 4. DOS plot of (a) compound **5** and (b) compound **6** indicating HOMO-LUMO gap.

3.3. Frontier molecular orbital: HOMO and LUMO.

The DFT method has been used to determine the HOMO and LUMO orbital diagrams. HOMO generally refers to the maximum amount of electron density in the part of the molecule where an electrophile can easily attack. From the following pictures (Figure 5), it can be seen that the LUMO parts are present in the alkyl chains and pyrimidine moieties of the uridine portion. In comparison, the HOMO part extends on the sugar (ribofuranose, glucopyranose, and hydroxyl group) part. Also, electronegative atoms, i.e., mainly oxygen atoms of those regions, are more likely to have HOMO orbitals.

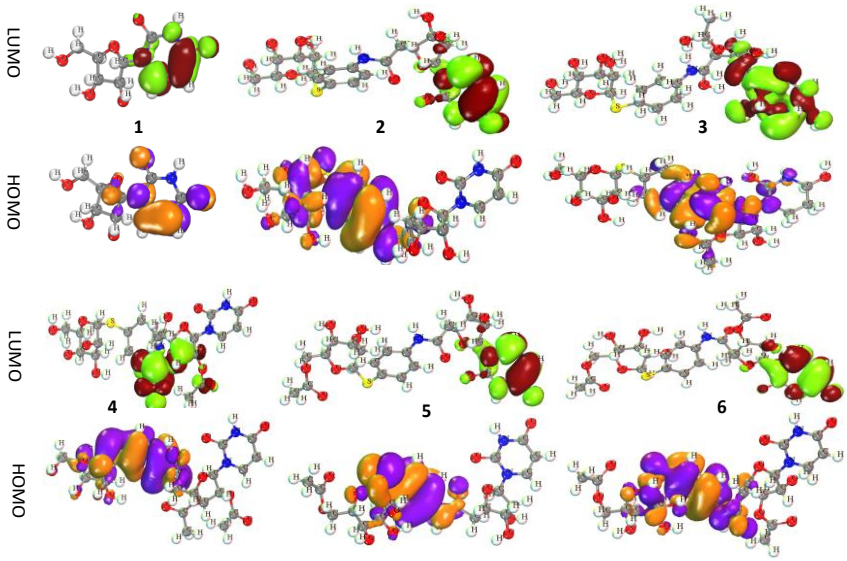

Figure 5. Frontier molecular orbitals diagram for HOMO and LUMO of glucoconjugates 2-6.

After analyzing their optimized structures, this study clearly showed this conceptual knowledge about HOMO from the frontier molecular orbital. On the other hand, the term LUMO refers to the lack of electrons where an electron-withdrawing group or nucleophilic group can easily be added. From Figure 5, it is seen that the LUMO of these molecules is associated with the alkyl group/part(s).

3.4. Molecular electrostatic potential (MEP).

Molecular electrostatic potential (MEP) correlates various physicochemical properties of compounds such as dipole moment, electronegativity, and partial charges especially MEP forecast the reactive electrophilic and nucleophilic sites of molecules. MEP is created in the space around a molecule by its nuclei and electrons (formed as static distributions of charge) It is a useful property for explaining and predicting its reactive behavior. Computationally predicted MEP of 1-6 and sofosbuvir are shown in Figure 6. The molecular MEP of 1-6 are predicted from their DFT optimized structures using the WebMo server [17].

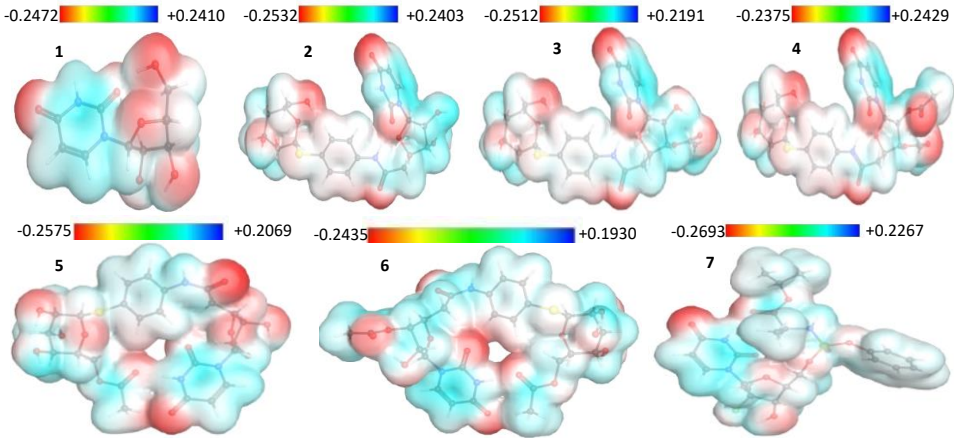

Figure 6. Molecular electrostatic potential (MEP) of uridine thioglucosides 2-6.

Traditionally, the lowest electrostatic potential energy value is indicated by red, representing the maximum negative area and favorable site for electrophilic attack. On the

other hand, the highest electrostatic potential energy value is represented by the blue zone in MEP, which indicates the maximum positive area and favorable site for nucleophilic attack. Again, the green color indicates zero potential areas. It is evident from Figure 6 that uridine (1), uridine thioglucosides 2-6, and sofosbuvir (7) possess almost similar red and blue zones indicating that these compounds are almost equally favorable for electrophilic reaction than nucleophilic attack. However, a critical observation showed their higher red zones compared to blue zones, informing their better electrophilic reaction.

3.5. Pharmacokinetics: drug-likeness study.

Optimal drug-likeness in compounds should be targeted in the early phases of drug research since it contributes to individual ADMET (absorption, distribution, metabolism, elimination, and toxicology), blood-brain barrier (BBB) penetration, and clearance. According to Lipinski rules (rule of five), drug-like molecules need to possess the five parameters such as drug molecule should have- (i) less than 5 hydrogen bond donors (HBD), (ii) less than 10 hydrogen bond acceptors (HBA), (iii) more than three number of rotatable bonds (NBR), (iv) molecular mass (MW) less than 500 Daltons, and (v) octanol-water partition coefficient (log Po/w) is not greater than 5 [44]. The HBD, HBA, NBR, MW, log Po/w, log S, and Lipinski rule violations of the glucofuranose compounds are presented in Table 2.

Table 2. Drug-likeness properties of 1-6.

Mol	HBD	HBA	NBR	TPSA (Å²)	Log Po/w	Log S (mg/ml)	Lipinski rule		MW
							Follow	Violation	
1	4	7	2	124.78	-1.67	-0.24	5	0	244.20
2	8	11	8	249.10	-1.69	-1.23	2	3	541.53
3	7	12	10	255.17	-1.48	-1.70	2	3	583.56
4	6	13	12	261.24	-1.27	-1.97	2	3	625.60
5	7	12	10	255.17	-1.71	-1.16	2	3	583.56
6	6	13	12	261.24	-1.31	-1.63	2	3	625.60
7	3	11	11	167.99	1.50	-3.27	3	2	529.45

7 = sofosbuvir; Log *S* scale: Insoluble<-10<poorly<-6<moderately<-4<soluble<-2<very soluble <0<highly soluble.

It is found that almost all uridine thioglucosides molecules 2-6 partially obeyed the Lipinski rule. Also, these compounds possess topological polar surface areas above 140 Å² like standard hepatitis virus drugs. The *n*-octanol/water partition coefficient (log Po/w) is a key physicochemical parameter for drug discovery, design, and development. It is indicated as the ratio of the concentration of the non-ionized compound at equilibrium between organic and aqueous phases. All the target compounds 2-6 have lower lipophilicity and higher water solubility than uridine (1) and standard drug sofosbuvir (7).

3.6. Pharmacokinetics: ADMET studies.

Pharmacokinetic (PK) drug testing is needed in preclinical efficacy species (typically mice) at the early stage of drug discovery to ensure whether a potential drug has the necessary exposure to achieve efficacy following *in vivo* dosing [59]. It mainly consists of ADMET (absorption, distribution, metabolism, excretion, and toxicity) and indicates what the body does to the drug. A very similar term PD (pharmacodynamics), outlines what the drug does to the body. Nowadays, both PK and PD can be predicted using any software. In the present study, pkCSM protocol (http://biosig.unimelb.edu.au) [52] was applied to predict ADMET of **1-6** and presented in Table 3.

Table 3. ADMET properties of uridine compound 1-7.

Drug	Absorption			Distribution		Metabolism	Excretion	Toxicity	
	C2P	HIA (%)	P-gpI	BBB (permeability)	CNS (permeability)	CYP3A4	TC	hERGI	LD_{50} (rat)
1	-0.224	36.543	No	-1.300	-4.043	No	0.669	No	1.896
2	0.597	9.562	No	-2.301	-4.332	No	0.151	No	2.631
3	-0.480	7.135	No	-2.297	-3.956	No	0.043	No	2.913
4	-0.427	12.755	No	-2.425	-3.949	No	0.008	No	3.190
5	-0.656	22.667	No	-2.248	-3.968	No	0.042	No	2.827
6	0.329	20.24	No	-2.244	-3.593	No	-0.066	No	3.042
7	0.458	62.676	No	-1.870	-4.316	No	-0.108	No	2.669

TC = total clearance and measured in log mL/min/kg; I = inhibitor; **7** = sofosbuvir.

Initially, absorption is predicted as Caco-2 permeability (C2P), human intestinal absorption (HIA), and P-glycoprotein inhibitor (P-gpI). Like sofosbuvir (7), all the compounds are found non-P-gpI. Their C2P and HIA are lower than the standard drug 7. The blood-brain barrier (BBB) and central nervous system (CNS) permeability represent the distribution of 1-7. BBB and CNS are found to be in good agreement with standard sofosbuvir. In terms of metabolism, all the compounds are not metabolic substrates of CYP3A4.

The uridine thioglucosides have slightly lower renal excretion as compared to **7**. Interestingly, all the compounds 1-6 have lower toxicity in terms of human ether-a-go-go-gene (hERG) and oral rat acute toxicity (LD_{50}) (Table 3). As these compounds are predicted as non-inhibitor of hERG, they should have fewer side effects (less or non-toxic). Thus, the uridine thioglucosides might be a safer drug to use.

3.7. Molecular docking: anti-hepatitis activities.

Molecular docking studies were conducted to validate the obtained pharmacological data [60] and provide evidence for the binding affinity of drug compounds 2-6 with proteins of Hepatitis C virus (HCV; 3su4) and Hepatitis B virus (HBV; 5e0i). Sofosbuvir is deliberately chosen as a standard drug due to its encouraging use in chronic HCV treatment and structural resemblance with the target compounds under investigation. Sofosbuvir (Figure 7) prevents HCV viral replication by binding with HCV polymerase's active site and preventing further replication of HCV genetic material.

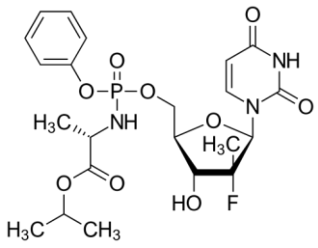

Figure 7. Structure of Sofosbuvir (7).

Several direct-acting antiviral agents (DAAs) for HCV target the essential 3su4 protease (NS3 protease, NS4A protein, or simply NS3/4A serine protease) and are approved by the FDA. Hence, at first, molecular docking of the uridine thioglucosides was conducted with 3su4 protease (HCV). The binding affinity and interactions, as shown in Table 4 and Table 5, all the compounds exhibited better binding affinities as compared to the uridine (1) and sofosbuvir (7, Figure 7). Compound 5 with two acetyl groups at the ribofuranose part showed the highest binding affinity (-8.1 kcal/mol), which was found higher than that of standard antiviral drug **7** (-6.8 kcal/mol).

Table 4. Binding energy and name of interacted ligand for Hepacivirus C (3su4).

Drug	Binding affinity (kcal/mol)	No. of H bond	No. of hydrophobic bond	No. of van der Waal bond	Total bonds
1	-6.2	5	2	Absent	7
2	-7.9	7	5	Absent	12
3	-7.4	6	4	Absent	10
4	-6.8	6	5	Absent	11
5	-8.1	3	3	Absent	6
6	-6.9	5	5	Absent	10
7	-6.8	3	6	Absent	9

* Standard docking score value is ≤-6.00 kcal/mol

Table 7 indicated that all the uridine-based drug compounds formed different hydrophilic and hydrophobic interactions with the 3su4 protein chain (Figure 8). It was reported that DAA-like telaprevir showed four hydrogen bonds with the amino acid residues present in the active site of the HCV NS3/4A protease [61]. These thioglucosides also showed several hydrogen bonds and non-bond interaction with this protease (Table 5).

Table 5. Protease 3su4 and ligands interaction with amino acid (AA) residues and their bond distance.

Drug	Hydrogen bond		Hydrophobic bond		Van der Waals bond
	Interacting residue of amino acid	Distance (Å)	Interacting residue of amino acid	Distance (Å)	
1	GLY-1137 LEU-1135 ALA-1157 LYS-1155 LYS-1136	3.12 2.79 3.04 3.54 3.60	ALA-1139 LYS-1136	5.31 4.94	Absent
2	ARG-127 GLY-123 LEU-15 LEU-16 TYR-118 SER-106 SER-106	3.02 3.60 2.93 2.43 3.01 2.73 2.87	PHE-122 PHE-24 TRP-102 TRP-102 PRO-25	4.69 4.71 5.68 4.60 4.96	Absent
3	ARG-127 LEU-16 LEU-140 TYR-118 SER-106 SER-106	3.01 2.69 3.15 2.89 2.75 2.61	PHE-24 PHE-24 PHE-122 PRO-25	3.98 5.11 4.82 5.04	Absent
4	LEU-16 LEU-119 TYR-118 TRP-102 SER-106 SER-106	2.00 2.66 2.77 3.05 2.77 2.74	PHE-24 PHE-24 PHE-122 PRO-25 PRO-25	5.02 4.40 4.85 5.40 4.91	Absent
5	LEU-119 THR-109 SER-106	2.33 3.40 3.86	PHE-24 PHE-122 TRP-102	5.21 4.99 5.41	Absent
6	ARG-127 LEU-119 TYR-118 TRP-102 TRP-102	3.10 3.75 2.70 3.19 2.64	PHE-24 PHE-122 TRP-102 LEU-119 ARG-127	5.10 5.25 5.11 5.22 4.36	Absent
7	THR-1040 SER-1037 ARG-1109	2.23 2.82 2.90	THR-1042 HIS-1110 HIS-1110 ALA-1007 ALA-1007 ILE-1035	3.92 4.69 4.62 3.89 5.43 5.40	Absent

Note: TRP = TRPptophan, ASP = Aspartic acid, GLU = Glutamic acid, LEU = Leucine, THR = Threonine, ASN = Asparagine, GLN = Glutamine, PHE = Phenylalanine, ILE = Isoleucine, ARG = Arginine, VAL = Valine, SER = Serine, PRO = Proline, GLY = Glycine, HIS = Histidine, LYS = Lysine, TRP = TRPosine, CYS = Cysteine, MET = Methionine.

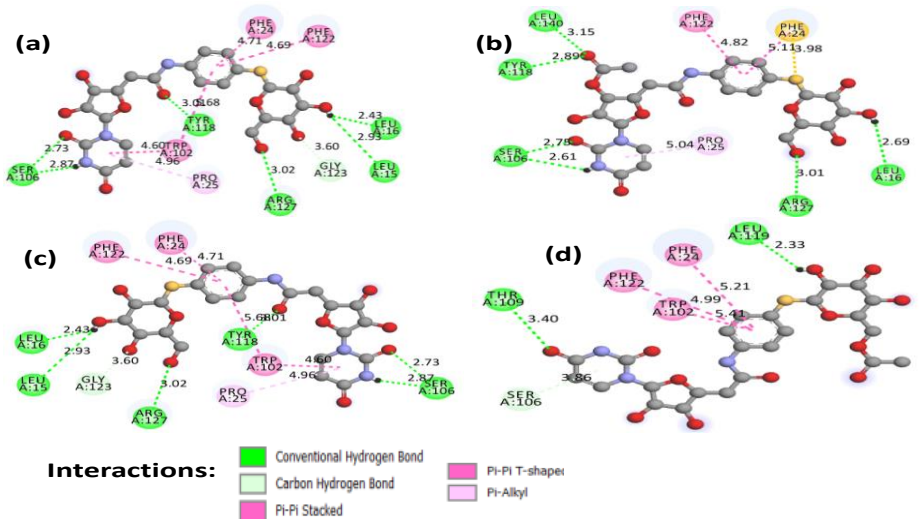

Figure 8. Interactions of molecules with amino acid residues: (a) 2 with 5e0i; (b) 3 with 5e0i; (c) 2 with 3su4; (d) 5 with 3su4.

Again, the HBV core protein is the major target for developing new therapies to treat HBV-infected patients. Hence, molecular docking was conducted with 5e0i, and the binding affinities of 1-7 are shown in Table 6. In both the cases (3su4 and 5e0i), the binding affinities for 2-6 were calculated higher than the standard anti-hepatitis drug sofosbuvir. Overall, the thioglucosides showed a better binding affinity with HBV protease (5e0i) than HCV (3su4). It should be noted that the target protein 5e0i with a 6-chain structure is the core protein of the HBV and is essential for HBV replication. So, it is an important target for antiviral drug discovery.

Table 6. Binding energy and name of interacted ligand for Hepacivirus B (5e0i).

Drug	Binding affinity (kcal/mol)	No. of H bond	No of hydrophobic bond	No of van der Waal bond	Total bonds
1	-6.0	5	2	Absent	7
2	-8.7	6	5	Absent	11
3	-8.7	6	4	Absent	10
4	-8.4	6	5	Absent	11
5	-7.9	3	3	Absent	6
6	-8.1	5	5	Absent	10
7	-8.0	7	6	Absent	13

* Standard docking score value is ≤-6.00 kcal/mol

The uridine thioglucosides 2-6 (-7.9 to -8.7 kcal/mol) showed better binding affinities than the uridine (1, -6.0 kcal/mol). The addition of the acetyl group at ribofuranose, glucopyranose, or both the parts did not change significant binding affinities with 5e0i. The best binding affinity was found for 2 and 3 (-8.7 kcal/mol), higher than antiviral sofosbuvir (-8.0 kcal/mol). The results were also supported by their good hydrogen bond and hydrophobic interaction with different amino acid residues of the protein chain of 5e0i (HBV; Table 7; Figure 8). Thus, further studies may establish these uridine-based thioglucosides as potential antiviral drugs, especially against HBV and HCV.

4. Conclusions

The available HCV and HBV antiviral therapeutics boceprevir, telaprevir, etc., cause severe side effects and long-term application of these drugs create drug resistance, which is a global health concern.

Table 7. Protease 5e0i and ligands interaction with amino acid (AA) residues and their bond distance.

Drug	Hydrogen bond		Hydrophobic bond		Van der Waals bond
	Interacting residue of amino acid	Distance (Å)	Interacting residue of amino acid	Distance (Å)	
1	ARG-28 LEU-31 GLU-43 LEU-42	3.17 1.87 1.98 1.98	LEU-31 ILE-59 ALA-35	5.08 5.04 4.53	Absent
2	AGR-127 LEU-15 LEU-16 TYR-118 SER-106 SER-106	3.02 2.93 2.43 3.01 2.73 2.87	PHE-122 PHE-24 TRP-102 TRP-102 PRO-25	4.69 4.71 5.68 4.60 4.96	Absent
3	ARG-127 LEU-16 LEU-140 TYR-118 SER-106 SER-106	3.01 2.69 3.15 2.89 2.75 2.61	PHE-24 PHE-24 PHE-122 PRO-25	3.98 5.11 4.82 5.04	Absent
4	LEU-16 LEU-119 TYR-118 TRP-102 SER-106 SER-106	2.00 2.66 2.77 3.05 2.77 2.74	PHE-24 PHE-24 PHE-122 PRO-25 PRO-25	5.02 4.40 4.85 5.40 3.05	Absent
5	LEU-119 THR-109 SER-106	2.33 3.40 3.86	PHE-24 PHE-122 TRP-102	5.21 5.41 4.99	Absent
6	ARG-127 LEU-119 TYR-118 TRP-102 TRP-102	3.10 3.75 2.70 3.19 2.64	LEU-119 ARG-127 PHE-122 PHE-24 TRP-102	5.22 4.36 5.25 5.10 5.11	Absent
7	AASP-29 THR-33 SER-106 TRP-102 TRP-102 TYR-118 LEU-140	2.76 2.50 3.50 3.15 3.26 2.95 3.02	PHE-24 PHE-122 PRO-25 ALA-137 ILE-139 ILE-139	4.90 4.91 4.12 4.49 4.24 3.90	Absent

Note: Short names of AA residues are mentioned in Table 5.

To develop more potent next-generation HCV and HBV protease inhibitors, several uridine-structured 4-aminophenyl 1-thioglucosides were docked against related proteins 3su4 and 5e0i, respectively. The thioglucosides showed a better binding affinity with HBV protease (5e0i) than HCV (3su4). In addition, all the thioglucosides 2-6 have a higher electrophilicity index, which indicates their stronger electrophilic nature than the standard drug sofosbuvir. The present drug-likeness, FMO, MEP, and molecular docking results and related study will help design uridine-based potential strategies to develop robust therapies against these deadly HCV and HBV soon.

Funding

This research was funded by Research and Publication Cell (University of Chittagong), COVID-19 Special 2021, 124/5.

Acknowledgments

The administrative and technical support from the Department of Chemistry, University of Chittagong, is highly acknowledged.

Conflicts of Interest

The authors declare no conflict of interest.

References

1. Pastuch-Gawolek, G.; Chaubey, B.; Szewczyk, B.; Krol, E. Novel thioglycosyl analogs of glycosyltransferase substrates as antiviral compounds against classical swine fever virus and hepatitis C virus. *Eur. J. Med. Chem.* **2017**, *137*, 247–262, https://doi.org/10.1016/j.ejmech.2017.05.051.
2. Breton, C.; Fournel-Gigleux, S.; Palcic, M.M. Recent structures, evolution and mechanisms of glycosyltransferases. *Curr. Opin. Struct. Biol.* **2012**, *22*, 540–549, https://doi.org/10.1016/j.sbi.2012.06.007.
3. Sato, T.; Hisashi, N.H. Beta-1,3-Glucosyltransferase (B3GALTL). In: *Handbook of Glycosyltransferases and Related Genes.* 2nd ed.; Taniguchi, N.; Honke, K.; Fukuda, M.; Narimatsu, H.; Yamaguchi, Y.; Angata, T. Eds.; Springer: Tokyo, Japan, **2014**; pp. 31-38.
4. Pastuch-Gawolek, G.; Bieg, T.; Szeja, W.; Flasz, J. 5-Amino-2-pyridyl 1-thioglycosides in synthesis of analogs of glycosyltransferases substrates. *Bioorg. Chem.* **2009**, *37*, 77–83, https://doi.org/10.1016/j.bioorg.2009.04.002.
5. Krol, E.; Pastuch-Gawolek, G.; Chaubey, B.; Brzuska, G.; Erfurt, K.; Szewczyk, B. Novel uridine glycoconjugates, derivatives of 4-aminophenyl 1-thioglycosides, as potential antiviral compounds. *Molecules* **2018**, *23*, https://doi.org/10.3390/molecules23061435
6. Guthrie, R.D.; Honeyman, J. *An Introduction to the Chemistry of Carbohydrates.* 3rd ed.; Clarendon Press: Oxford, UK, **1968**.
7. Ei-Laithy, H.M.; Shoukry, O.; Mahran, L.G. Novel sugar esters proniosomes for transdermal delivery of vinpocetine: Preclinical and clinical studies. *Eur. J. Pharm. Biopharm*. **2011**, *77*, 43–55, https://doi.org/10.1016/j.ejpb.2010.10.011.
8. Matin, M.M.; Chakraborty, P.; Alam, M.S.; Islam, M.M.; Hanee, U. Novel mannopyranoside esters as sterol 14α-demethylase inhibitors: Synthesis, PASS predication, molecular docking, and pharmacokinetic studies. *Carbohydr. Res*. **2020**, *496*, https://doi.org/10.1016/j.carres.2020.108130.
9. Moyer, B.G.; Pfeffer, P.E.; Moniot, J.L.; Shamma, M.; Gustine, D.L. Corollin, coronillin and coronarian: Three new 3-nitropropanoyl-d-glucopyranoses from Coronilla varia. *Phytochem*. **1977**, *16*, 375-377, http://dx.doi.org/10.1016/0031-9422(77)80068-X.
10. Dhavale, D.D.; Matin, M.M. Selective sulfonylation of 4-C-hyroxymethyl-β-L-threo-pento-1,4-furanose: Synthesis of bicyclic diazasugars. *Tetrahedron* **2004**, *60*, 4275–4281, https://doi.org/10.1016/j.tet.2004.03.034.
11. Godehard, S.P.; Müller, H.; Badenhorst, C.P.S.; Stanetty, C.; Suster, C.; Mihovilovic, M.D.; Bornscheuer, U.T. Efficient acylation of sugars and oligosaccharides in aqueous environment using engineered acyltransferases. *ACS Catal.* **2021**, *11*, 2831-2836, https://doi.org/10.1021/acscatal.1c00048.
12. Matin, M.M.; Bhattacharjee, S.C.; Chakraborty, P.; Alam, M.S. Synthesis, PASS predication, *in vitro* antimicrobial evaluation and pharmacokinetic study of novel *n*-octyl glucopyranoside esters. *Carbohydr. Res.* **2019**, *485*, https://doi.org/10.1016/j.carres.2019.107812.
13. Devi, P.; Matin, M.M.; Bhuiyan, M.M.H.; Hossain, M.E. Synthesis, and spectral characterization of 6-*O*-octanoyl-1,2-*O*-isopropylidene-α-D-glucofuranose derivatives. *J. Turk. Chem. Soc. Sect. A: Chem.* **2021**, *8*, 1003-1024, https://doi.org/10.18596/jotcsa.929996.
14. Matin, M.M.; Islam, N.; Siddika, A.; Bhattacharjee, S.C. Regioselective synthesis of some rhamnopyranoside esters for PASS predication, and ADMET studies. *J. Turk. Chem. Soc. Sect. A: Chem.* **2021**, *8*, 363–374, https://doi.org/10.18596/jotcsa.829658.
15. Jäger, M.; Adriaan Minnaard, A.J. Regioselective modification of unprotected glycosides. *Chem. Commun.* **2016**, *52*, 656-664, https://doi.org/10.1039/C5CC08199H.
16. Matin, M.M.; Bhuiyan, M.M.H.; Kabir, E.; Sanaullah, A.F.M.; Rahman, M.A.; Hossain, M.E.; Uzzaman, M. Synthesis, characterization, ADMET, PASS predication, and antimicrobial study of 6-*O*-lauroyl mannopyranosides. *J. Mol. Struct.* **2019**, *1195*, 189–197, https://doi.org/10.1016/j.molstruc.2019.05.102.
17. Matin, M.M.; Iqbal, M.Z. Methyl 4-*O*-(2-chlorobenzoyl)-α-L-rhamnopyranosides: Synthesis, characterization, and thermodynamic studies. *Orbital: Electron. J. Chem.* **2021**, *13*, 19–27.
18. Matin, M.M.; Ibrahim, M.; Rahman, M.S. Antimicrobial evaluation of methyl 4-*O*-acetyl-α-L-rhamnopyranoside derivatives. *Chittagong Univ. J. Biol. Sci.* **2008**, *3*, 33–43, http://dx.doi.org/10.3329/cujbs.v3i1.13404.
19. Matin, M.M.; Bhuiyan, M.M.H.; Azad, A.K.M.S.; Rashid, M.H.O. Synthesis of 6-O-stearoyl-1,2-O-isopropylidene-α-D-gluco-furanose derivatives for antimicrobial evaluation. *J. Phys. Sci.* **2015**, *26*, 1–12.
20. Gumel, A.M.; Annuar, M.S.M.; Heidelberg, T.; Chisti, Y. Lipase mediated synthesis of sugar fatty acid esters. *Process Biochem*. **2011**, *46*, 2079–2090, https://doi.org/10.1016/j.procbio.2011.07.021.
21. Perinelli, D.R.; Lucarini, S.; Fagioli, L.; Campana, R.; Vllasaliu, D.; Duranti, A.; Casettari, L.; Lactose oleate as new biocompatible surfactant for pharmaceutical applications. *Eur. J. Pharm. Biopharm*. **2018**, *124*, 55–62, https://doi.org/10.1016/j.ejpb.2017.12.008.

22. Dhavale, D.D.; Matin, M.M.; Sharma, T.; Sabharwal, S.G. Synthesis and evaluation of glycosidase inhibitory activity of octahydro-2*H*-pyrido[1,2-a]pyrimidine and octahydro-imidazo[1,2-a]pyridine bicyclic diazasugars. *Bioorg. Med. Chem.* **2004**, *12*, 4039–4044, https://doi.org/10.1016/j.bmc.2004.05.030.
23. Ren, B.; Zhang, L.; Zhang, M. Progress on selective acylation of carbohydrate hydroxyl groups. *Asian J. Org. Chem.* **2019**, *8*, 1813–1823, https://doi.org/10.1002/ajoc.201900400.
24. Battaglia, S.; De Santis, S.; Rutigliano, M.; Sallustio, F.; Picerno, A.; Frassanito, M.A.; Schaefer, I.; Vacca, A.; Moschetta, A.; Seibel, P.; Battaglia, M.; Villani, G. Uridine and pyruvate protect T cells' proliferative capacity from mitochondrial toxic antibiotics: a clinical pilot study. *Sci. Rep.* **2021**, *11*, https://doi.org/10.1038/s41598-021-91559-8,
25. Rahman, M.A.; Matin, M.M.; Kumer, A.; Chakma, U.; Rahman, M.R. Modified D-glucofuranoses as new black fungus protease inhibitors: Computational screening, docking, dynamics, and QSAR study. *Phys. Chem. Res.* **2022**, *10*, 189-203.
26. Matin, M.M.; Bhuiyan, M.H.; Hossain, M.M.; Roshid, M.H.O. Comparative antibacterial activities of some monosaccharide and disaccharide benzoates. *Orbital: Electron. J. Chem.* **2015**, *7*, 160-167.
27. Serpi, M.; Ferrari, V.; Pertusati, F. Nucleoside derived antibiotics to fight microbial drug resistance: new utilities for an established class of drugs? *J. Med. Chem.* **2016**, *59*, 10343−10382, https://doi.org/10.1021/acs.jmedchem.6b00325.
28. Zhang, Y.; Guo, Y.; Xie, C.; Fang, J. Uridine metabolism and its role in glucose, lipid, and amino acid homeostasis. *Biomed. Res. Int.* **2020**, *2020*, https://doi.org/10.1155/2020/7091718.
29. Thatipamula, R.K.; Narsimha, S.; Battula, K.; Chary, V.R.; Mamidala, E.; Reddy, N.V. Synthesis, anticancer and antibacterial evaluation of novel (isopropylidene) uridine-[1,2,3]triazole hybrids. *J. Saudi Chem. Soc.* **2017**, *21*, 795-802, https://doi.org/10.1016/j.jscs.2015.12.001.
30. Shelton, J.; Lu, X.; Hollenbaugh, J.A.; Cho, J.H.; Amblard, F.; Schinazi, R.F. Metabolism, biochemical actions, and chemical synthesis of anticancer nucleosides, nucleotides, and base analogs. *Chem. Rev.* **2016**, *116*, 14379−14455, https://doi.org/10.1021/acs.chemrev.6b00209.
31. Matin, M.M.; Uzzaman, M.; Chowdhury, S.A.; Bhuiyan, M.M.H. In vitro antimicrobial, physicochemical, pharmacokinetics, and molecular docking studies of benzoyl uridine esters against SARS-CoV-2 main protease. *J. Biomol. Struct. Dyn.* **2020**, https://doi.org/10.1080/07391102.2020.1850358.
32. Carlezon, W.A.; Mague Jr, S.D.; Parow, A.M; Stoll, A.L.; Cohen, B.M.; Renshaw, P.F. Antidepressant-like effects of uridine and omega-3 fatty acids are potentiated by combined treatment in rats. *Biol. Psychiatry* **2005**, *57*, 343–350, https://doi.org/10.1016/j.biopsych.2004.11.038.
33. Siegel, D.; Hui, H.C.; Doerffler, E.; Clarke, M.O.; Chun, K.; Zhang, L.; Neville, S.; Carra, E.; Lew, W.; Ross, B.; Wang, Q.; Wolfe, L.; Jordan, R.; Soloveva, V.; Knox, J.; Perry, J.; Perron, M.; Stray, K.M.; Barauskas, O.; Feng, J.Y.; Xu, Y.; Lee, G.; Rheingold, A.L.; Ray, A.S.; Bannister, R.; Strickley, R.; Swaminathan, S.; Lee, W.A.; Bavari, S.; Cihlar, T.; Lo, M.K.; Warren, T.K.; Mackman, R.L. Discovery and synthesis of a phosphoramidate prodrug of a Pyrrolo[2,1-f][triazin-4-amino] adenine C-nucleoside (GS-5734) for the treatment of ebola and emerging viruses. *J. Med. Chem.* **2017**, *60*, 1648–1661, https://doi.org/10.1021/acs.jmedchem.6b01594.
34. Susilo, R. (Koln, DE). Pharmaceutically active uridine esters, United States, Trommsdorff GmbH & Co. KG Arzeneimittel (Alsdorf, DE). 7417034, **2008.**
35. Pedersen, L.L.; Turco, S.J. Galactofuranose metabolism: a potential target for antimicrobial chemotherapy. *Cell. Mol. Life Sci.* **2003**, *60*, 259–266, https://doi.org/10.1007/s000180300021.
36. von Itzstein, M. Disease-associated carbohydrate-recognising proteins and structure-based inhibitor design. *Curr. Opin. Struct. Biol.* **2008**, *18*, 558–566, https://doi.org/10.1016/j.sbi.2008.07.006.
37. Pastuch-Gawolek, G.; Plesniak, M.; Komor, R.; Byczek-Wyrostek, A.; Erfurt, K.; Szeja, W. Synthesis and preliminary biological assay of uridine glycoconjugate derivatives containing amide and/or 1,2,3-triazole linkers. *Bioorg. Chem.* **2017**, *72*, 80–88, http://dx.doi.org/10.1016/j.bioorg.2017.03.015.
38. Palumbo, E. Pegylated interferon and Ribavirin treatment for Hepatitis C Virus infection. *Ther. Adv. Chronic Dis.* **2011**, *2*, 39–45, https://doi.org/10.1177/2040622310384308.
39. Barth, H. Hepatitis C virus: Is it time to say goodbye yet? Perspectives and challenges for the next decade. *World J. Hepatol.* **2015**, *7*, 725–737, https://doi.org/10.4254/wjh.v7.i5.725.
40. Dhavale, D.D.; Matin, M.M.; Sharma, T.; Sabharwal, S.G. N-Hydroxyethyl-piperidine and –pyrrolidine homoazasugars: preparation and evaluation of glycosidase inhibitory activity. *Bioorg. Med. Chem.* **2003**, *11*, 3295–3305, https://doi.org/10.1016/S0968-0896(03)00231-1.
41. Connolly, G.P.; Duley, J.A. Uridine and its nucleotides: biological actions, therapeutic potentials. *Trends Pharmacol. Sci.* **1999**, *20*, 218–225, https://doi.org/10.1016/s0165-6147(99)01298-5.
42. Peccatori, F.A.; Lambertini, M.; Scarfone, G.; Pup, L.D.; Codacci-Pisanelli, G. Biology, staging, and treatment of breast cancer during pregnancy: reassessing the evidences. *Cancer Biol Med.* **2018**, *15*, 6-13, https://doi.org/10.20892/j.issn.2095-3941.2017.0146.
43. Matin, M.M.; Hasan, M.S.; Uzzaman, M.; Bhuiyan, M.M.H.; Kibria, S.M.; Hossain, M.E.; Roshid, M.H.O. Synthesis, spectroscopic characterization, molecular docking, and ADMET studies of mannopyranoside esters as antimicrobial agents. *J. Mol. Struct.* **2020**, *1222*, https://doi.org/10.1016/j.molstruc.2020.128821.

44. Islam, F.; Rahman, M.R.; Matin, M.M. The effects of protecting and acyl groups on the conformation of benzyl α-L-rhamnopyranosides: An in silico study. *Turk. Comp. Theo. Chem.* **2021**, *5*, 39–50, https://doi.org/10.33435/tcandtc.914768.
45. Matin, M.M.; Nath, A.R.; Saad, O.; Bhuiyan, M.M.H.; Kadir, F.A.; Abd Hamid, S.B.; Alhadi, A.A.; Ali, M.E.; Yehye, W.A. Synthesis, PASS-predication and in vitro antimicrobial activity of benzyl 4-*O*-benzoyl-α-L-rhamnopyranoside derivatives. *Int. J. Mol. Sci.* **2016**, *17*, https://doi.org/10.3390/ijms17091412.
46. Frisch, M.J.; Trucks, G.W.; Schlegel, H.B.; Scuseria, G.E.; Robb, M.A.; Cheeseman, J.R.; Scalmani, G.; Barone, V.; Mennucci, B.; Petersson, G.A.; Nakatsuji, H.; Caricato, M.; Li, X.; Hratchian, H.P.; Izmaylov, A.F.; Bloino, J.; Zheng, G.; Sonnenberg, J.L.; Hada, M.; Ehara, M.; Toyota, K.; Fukuda, R.; Hasegawa, J.; Ishida, M.; Nakajima, T.; Honda, Y.; Kitao, O.; Nakai, H.; Vreven, T.; Montgomery Jr, J.A.; Peralta, J. E.; Ogliaro, F.; Bearpark, M.; Heyd, J.J.; Brothers, E.; Kudin, K.N.; Staroverov, V.N.; Keith, T.; Kobayashi, R.; Normand, J.; Raghavachari, K.; Rendell, A.; Burant, J. C.; Iyengar, S.S.; Tomasi, J.; Cossi, M.; Rega, N.; Millam, J.M.; Klene, M.; Knox, J.E.; Cross, J.B.; Bakken, V.; Adamo, C.; Jaramillo, J.; Gomperts, R.; Stratmann, R.E.; Yazyev, O.; Austin, A.J.; Cammi, R.; Pomelli, C.; Ochterski, J.W.; Martin, R.L.; Morokuma, K.; Zakrzewski, V.G.; Voth, G.A.; Salvador, P.; Dannenberg, J.J.; Dapprich, S.; Daniels, A.D.; Farkas, O.; Foresman, J.B.; Ortiz, J.V.; Cioslowski, J.; Fox, D.J. Gaussian 09W, Revision D.01, Gaussian, Inc, Wallingford CT, **2013**.
47. Becke, A.D. Density-functional thermochemistry. III. The role of exact exchange. *J. Chem. Phys.* **1993**, *98*, 5648-5652, https://doi.org/10.1063/1.464913 .
48. Ditchfield, R.; Hehre, W.J.; Pople, J.A. Self-Consistent Molecular Orbital Methods. 9. Extended Gaussian-type basis for molecular-orbital studies of organic molecules. *J. Chem. Phys.* **1971**, *54*, 724-728, http://dx.doi.org/10.1063/1.1674902.
49. Hehre, W.J.; Ditchfield, R.; Pople, J.A. Self-Consistent Molecular Orbital Methods. 12. Further extensions of Gaussian-type basis sets for use in molecular-orbital studies of organic-molecules. *J. Chem. Phys.* **1972**, *56*, 2257-2261, http://dx.doi.org/10.1063/1.1677527
50. Matin, M.M.; Chakraborty, P. Synthesis, spectral and DFT characterization, PASS predication, antimicrobial, and ADMET studies of some novel mannopyranoside esters. *J. Appl. Sci Process Eng.* **2020**, *7*, 572-586, https://doi.org/10.33736/jaspe.2603.2020.
51. Daina, A.; Michielin, O.; Zoete, V. SwissADME: a free web tool to evaluate pharmacokinetics, drug-likeness and medicinal chemistry friendliness of small molecules. *Sci. Rep.* **2017**, *7*, 1–13, https://doi.org/10.1038/srep42717.
52. Han, Y.; Zhang J.; Hu, C. Q.; Zhang Ma X. B.; Zhang, P. In silico ADME and toxicity prediction of Ceftazidime and its impurities. *Front. Pharmacol.* **2019**, *10*, http://dx.doi.org/10.3389/fphar.2019.00434.
53. Ramos, J. Introducción a Materials Studio en la Investigación Química y Ciencias de los Materiales. **2020**.
54. Muhammad, D.; Matin, M.M.; Miah, S.M.R.; Devi, P. Synthesis, antimicrobial, and DFT studies of some benzyl 4-O-acyl-α-L-rhamnopyranosides. *Orbital: Electron. J. Chem.* **2021**. *13*, 250–258.
55. DeLano, W.L. The PyMOL ” ’user’s manual. **2002**. http://www.pymol.org.
56. Ragusa, G.; Bencivenni, S.; Morales, P.; Callaway, T.; Hurst, D.P.; Asproni, B.; Merighi, S.; Loriga, G.; Pinna, G.A.; Reggio, P.H.; Gessi, S.; Murineddu, G. Synthesis, pharmacological evaluation and docking studies of novel pyridazinone-based cannabinoid receptor type-2 ligands. *ChemMedChem* **2018**, *13*, 1102-1114, https://doi.org/10.1002/cmdc.201800152.
57. AS Inc. Discovery Studio Modeling Environment, Release 4.0. [Online].
58. Lee, C.; Yang, W.; Parr, R.G. Development of the Colle-Salvetti correlation-energy formula into a functional of the electron density. *Physics Rev.* **1988**, *B37*, 785–789, https://doi.org/10.1103/PhysRevB.37.785.
59. Islam, N.; Islam, M.D.; Rahman, M.R.; Matin, M.M. Octyl 6-*O*-hexanoyl-β-D-glucopyranosides: Synthesis, PASS, antibacterial, in silico ADMET, and DFT studies. *Curr. Chem. Lett.* **2021**, *10*, 413–426, https://doi.org/10.5267/j.ccl.2021.5.003.
60. Nainu, F.; Masyita, A.; Bahar, M.A.; Raihan, M.; Prova, S.R.; Mitra, S.; Emran, T.B.; Simal-Gandara, J. Pharmaceutical prospects of bee products: Special focus on anticancer, antibacterial, antiviral, and antiparasitic properties. *Antibiotics* **2021**, *10*, https://doi.org/10.3390/antibiotics10070822.
61. Abuelizz, H.A.; Marzouk, M.; Bakheit, A.H.; AlSalahi, R. Investigation of some benzoquinazoline and quinazoline derivatives as novel inhibitors of HCVNS3/4A protease: biological, molecular docking and QSAR studie. *RSC Adv.* **2020**, *10*, 35820-35830, https://doi.org/10.1039/D0RA05604A.